CANADIAN APPLIED
MATHEMATICS QUARTERLY
Volume 11, Number 2, Summer 2003

CONSIDERATIONS ON YIELD, NUTRIENT UPTAKE, CELLULAR GROWTH, AND COMPETITION IN CHEMOSTAT MODELS

JULIEN ARINO, SERGEI S. PILYUGIN
AND GAIL S. K. WOLKOWICZ

ABSTRACT. We investigate some properties of a very general model of growth in the chemostat. In the classical models of the chemostat, the function describing cellular growth is assumed to be a constant multiple of the function modeling substrate uptake. The constant of proportionality is called the growth yield constant. Here, this assumption of a constant describing growth yield is relaxed. Instead, we assume that the relationship between uptake and growth might depend on the substrate concentration and hence that the yield is variable.

We obtain criteria for the stability of equilibria and for the occurrence of a Hopf bifurcation. In particular, a Hopf bifurcation can occur if the uptake function is unimodal. Then, in this setting, we consider competition in the chemostat for a single substrate, in order to challenge the principle of competitive exclusion.

We consider two examples. In the first, the function describing the growth process is monotone and in the second it is unimodal. In both examples, in order to obtain a Hopf bifurcation, one of the competitors is assumed to have a variable yield, and its "uptake" is described by a unimodal function. However, the interpretation is different in each case. We provide a necessary condition for strong coexistence and a sufficient condition that guarantees the extinction of one or more species. We show numerically by means of bifurcation diagrams and simulations, that the competitive exclusion principle can be breached resulting in oscillatory coexistence of more than one species, that competitor-mediated coexistence is possible, and that these simple systems can have very complicated dynamics.

1 Introduction Numerous papers deal with the growth of microorganisms in the chemostat. Most originate from bioengineering and microbiology, where the chemostat finds a wide variety of applications, from

theoretical studies of bacteria to the use of bacteria in biological waste decomposition and water purification (see, *e.g.*, [**10, 36**]). As well as being an experimental system that generates reproducible results, it has been modeled extensively with good success. When browsing the corpus of literature dedicated to modeling the chemostat, it appears that although approaches and applications are varied, most of the models rely on a simple relationship between two fundamental processes, nutrient uptake and cellular growth. In particular, in most models these processes are assumed to be proportional. The constant of proportionality is referred to as the growth yield constant or yield constant.

The notion of yield dates from the beginning of continuous bacterial culture, and is for example defined by Monod [**35**] as the ratio K of the amount of bacterial substance formed per amount of limiting nutrient utilized. He notes that if the growth is expressed as "standard" cell concentration, then $1/K$ represents the amount of limiting nutrient used up in the formation of a "standard" cell. He also notes that the yield has, for a given strain and a given compound and under similar conditions, a remarkable degree of stability and reproducibility. But this reasoning is based on the assumption of constant yield.

In most of the early models of microbial growth in the chemostat, besides assuming constant yield, it was assumed that growth was a monotone increasing function of substrate concentration. However, for some organisms, high concentrations of substrate can be detrimental, as was pointed out in 1925 by Briggs and Haldane [**7**]. See also [**43**] for a comprehensive review of the mechanisms involved. Inhibition was subsequently incorporated into models of bacterial growth (see, *e.g.*, [**3, 16**]). Attempting to fit experimental data, many authors have used different functional forms to model inhibition (see, *e.g.*, [**14, 33, 39**]).

Under the assumption of constant yield, mathematical models predict that there can be no sustained oscillations (see, *e.g.*, [**9, 23, 41, 45**]). Since such oscillations have been observed in experiments (see, *e.g.*, [**15**] for Arthrobacter globiformis and [**27**] for Lactobacillus plantarum), it is then useful to find models that reproduce these oscillations.

With this in mind, we explore models involving variable yield. In the case of batch experiments, it was shown [**29**] that oscillatory solutions occur only if the yield is a function of both the substrate and the cell concentration. In continuous culture, this is not necessary, and most of the work has focused on the simpler assumption of a substrate dependent yield. Different explanations can be given for this dependence. In the case of chemical reactors, the yield is obtained from mass balance equations. For biological reactors, it is more complicated. See [**42**] for

a recent review of various thermodynamical models. For a description of how units of substrate are converted into units for cellular (bio)mass, see [**36,** p. 28–38].

The earliest model considering a more accurate relationship between uptake and growth was developed by Koga and Humphrey [**24**]. They introduce a respiration coefficient, R. They note that when respiration is considered, the observed yield coefficient Y_{obs} is given by $1/Y_{obs} = 1/Y + R/\mu(S)$, where Y is a constant yield coefficient and $\mu(S)$ is the specific growth rate of the microorganisms. In subsequent work on the subject, [**11, 12, 17**] assume that growth and uptake are related through a linear function of the substrate concentration. In [**2, 38, 37**], linear and nonlinear functions modeling yield are considered and conditions are derived for the existence of a Hopf bifurcation.

It is a difficult task to determine which part of the dynamics stems from the "higher" level processes that are modeled, and which part stems from the nature of the hypotheses made on nutrient uptake and cellular growth. The objective of this paper is to explore the dynamics resulting from the different ways of modeling variable yield in the chemostat model. We review the commonly used methods describing uptake and growth, and study their interplay. To do this, we consider that the *uptake*, *i.e.*, the process through which a cell absorbs nutrient, can be different from *growth*, *i.e.*, the process through which a cell transforms the uptaken nutrient into biomass. However, we do not consider the effect of delay. We also do not consider long term nutrient storage directly.

The rest of this paper is organized as follows. In Section 2, we consider a very general model of single species growth in the chemostat and first restrict our attention to what all such models have in common. We give preliminary results, and in particular, show that the behavior of chemostat models about the washout equilibrium point is generic. We are able to deal with the local stability analysis in this very general setting as well as some global properties of the model. Then we look for differences in the dynamics based on differences in the monotonicity assumptions on the nutrient uptake and cellular growth and show that under certain assumptions Hopf bifurcation is possible, whereas under other assumptions it is not. In Section 3, we briefly discuss the yield term and give different interpretations justifying a substrate dependent yield function. In Section 4, we extend the model to the case of competing species. We provide a necessary condition for strong coexistence and a sufficient condition for the extinction of a population. We give numerical evidence indicating that, unlike in the constant yield case,

assuming a variable yield can lead to rather complicated dynamics and give numerical evidence that indicates that the principle of competitive extinction need not hold and that competitor-mediated coexistence seems to be possible.

2 The general model for single species growth in a chemostat Consider the following model of a chemostat in which a microbial species, with concentration (or biomass) at time t denoted $x(t)$, consumes a single substrate with concentration $S(t)$ at time t.

$$\frac{dS}{dt} = D(S^0 - S) - xu(S), \tag{1a}$$

$$\frac{dx}{dt} = x\left(g(S) - D_1\right), \tag{1b}$$

$$S(0) \geq 0, \quad x(0) \geq 0.$$

S^0 denotes the substrate concentration in the input feed, and D denotes the dilution rate. We assume only that $D_1 > 0$ and we make no assumption on the relative values of D and D_1. However, the most common interpretation for D_1 is that it is the sum of the dilution rate and the species specific death rate. Substrate is consumed by cells at the rate $u(S(t))$. This results in growth of the cellular biomass at the rate $g(S(t))$. The functions u and g are assumed to be continuously differentiable. The uptake function $u(S)$ is further assumed to satisfy $u(0) = 0$. By this, we mean that if there is no substrate in the environment, then there is no substrate uptake. As mentioned earlier, we do not model storage of nutrient directly and so in the absence of substrate, we assume that there is no growth so that $g(0) = 0$. Otherwise, $u(S)$ and $g(S)$ are positive for $S > 0$. Finally, we assume that each one of these functions is either monotone increasing or unimodal.

2.1 Local analysis The washout equilibrium, $E_0 \equiv (S^0, 0)$, always exists.

Condition 2.1. $E^* \equiv (S^*, x^*) = \left(S^*, \dfrac{D(S^0 - S^*)}{u(S^*)}\right)$, *where* S^* *is any solution of*

$$g(S) = D_1 \tag{2}$$

is a feasible positive equilibrium if, and only if, $S^* < S^0$.

In what follows, we restrict our attention to functions $u(S)$ and $g(S)$ that are either monotone increasing or initially monotone increasing and unimodal. Thus, there are at most two values of S that satisfy (2). They are denoted $\lambda, \mu \in \overline{\mathbb{R}}$, with $\lambda < \mu$. We adopt the convention that $\mu = \infty$ if (2) has only one solution, and $\lambda = \infty$ if (2) has no solution. Therefore, S^* must equal either λ or μ. We refer to E^* as E^*_λ or E^*_μ when it is necessary to make the distinction. See Figure 1.

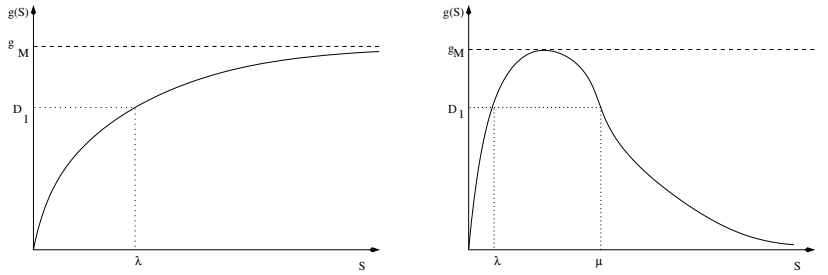

(a) (b)

FIGURE 1: Definition of λ and μ, in the case of (a) monotone growth ($\mu = \infty$); (b) nonmonotone growth.

We are not aware of any experimental evidence of growth or uptake processes limited by a single substrate that exhibit more complicated behavior (such as two-humped responses). A similar analysis for more complicated functions is however possible, but involves treating more cases.

The Jacobian matrix evaluated at an arbitrary point (S, x) is given by

$$\begin{bmatrix} -D - u'(S)x & -u(S) \\ g'(S)x & g(S) - D_1 \end{bmatrix}. \tag{3}$$

Thus, the Jacobian matrix evaluated at the washout equilibrium, E_0, is given by

$$\begin{bmatrix} -D & -u(S^0) \\ 0 & g(S^0) - D_1 \end{bmatrix}. \tag{4}$$

Condition 2.2. *The washout equilibrium, E_0, is locally asymptotically stable if $g(S^0) - D_1 < 0$.*

Evaluated at a positive equilibrium, E^*, the Jacobian matrix is

$$\begin{bmatrix} -D - u'(S^*)x^* & -u(S^*) \\ g'(S^*)x^* & 0 \end{bmatrix}. \tag{5}$$

Thus, $\det(J) = u(S^*)g'(S^*)x^*$ and $\mathrm{Tr}(J) = -D - u'(S^*)x^*$. Since $D, u, (S)$ and x^* are positive, by the Routh-Hurwitz criterion, we obtain the following condition.

Condition 2.3. *A feasible positive equilibrium, E^*, is locally asymptotically stable if the following two inequalities are satisfied simultaneously:*

$$g'(S^*) > 0, \qquad \textit{and} \qquad u'(S^*) > -\frac{u(S^*)}{S^0 - S^*}. \tag{6}$$

Another consequence of (5) is that the existence of complex eigenvalues, *i.e.*, oscillations (both damped and sustained), is determined by the following condition, which follows directly from the characteristic polynomial of (5).

Condition 2.4. *The linearization of* (1) *about a feasible positive equilibrium, E^*, has complex eigenvalues if, and only if, $(D + u'(S^*)x^*)^2 < 4u(S^*)g'(S^*)x^*$.*

This implies that there are no oscillations in a neighborhood of a positive equilibrium, E^*, if $g'(S^*) < 0$.

Condition 2.5. *The eigenvalues of the linearization* (5) *of system* (1) *about a positive equilibrium, E^*, are purely imaginary if, and only if,*

$$g'(S^*) > 0, \qquad \textit{and} \qquad u'(S^*) = -\frac{u(S^*)}{S^0 - S^*}, \tag{7}$$

Thus, a Hopf bifurcation of a locally asymptotically stable equilibrium point can only occur at an equilibrium, E^*_λ, since it is necessary that $u'(S^*) < 0$ and $g'(S^*) > 0$. Since the bifurcation requires g to be increasing at S^*, it follows that S^* must equal λ, not μ.

Select one of the parameters in the model as the bifurcation parameter and call it α.

Theorem 2.6. *Assume that there exists $\alpha = \alpha_c$, the critical value of α, such that $x^*_{\alpha_c} u'(\lambda_{\alpha_c}) + D = 0$. System (1) undergoes a Hopf bifurcation at $E^*_{\lambda_{\alpha_c}} = (\lambda_{\alpha_c}, x_{\alpha_c})$ if $g'(\lambda_{\alpha_c}) > 0$ and*

$$\frac{d}{d\alpha}\left(-Dx^*(\alpha)u'(S^*(\alpha))\right)\Big|_{\alpha=\alpha_c} \neq 0. \tag{8}$$

This bifurcation is supercritical if $C_{\mathcal{H}}$ defined by

$$C_{\mathcal{H}} \equiv -u(\lambda_{\alpha_c})g'(\lambda_{\alpha_c})u'''(\lambda_{\alpha_c}) + u''(\lambda_{\alpha_c})(u'(\lambda_{\alpha_c})g'(\lambda_{\alpha_c}) + u(\lambda_{\alpha_c})g''(\lambda_{\alpha_c}))$$

is negative, and subcritical if $C_{\mathcal{H}} > 0$.

Equivalently, the bifurcation is supercritical if the sign of

$$\hat{C}_{\mathcal{H}} \equiv h'''(\lambda_{\alpha_c})u(\lambda_{\alpha_c}) + 2h''(\lambda_{\alpha_c})u'(\lambda_{\alpha_c}) - \frac{h''(\lambda_{\alpha_c})g''(\lambda_{\alpha_c})u(\lambda_{\alpha_c})}{g'(\lambda_{\alpha_c})}$$

is negative, and subcritical if it is positive, where $h(S) = (S^0 - S)D/u(S)$, the S-isocline.

The proof of this result follows from the formula derived in Marsden and McCracken [**34**] and is postponed to Appendix 5. Another technique for determining the criticality of the Hopf bifurcation in this context is to use the divergence criterion as in [**38**] or the rescaling method as in [**37**].

2.2 Global analysis

2.2.1 *Boundedness of solutions.*

Lemma 2.7. *Both the nonnegative cone and the interior of the nonnegative cone are positively invariant under the flow of* (1).

Proof. The line $\{S \geq 0, x = 0\}$ is invariant under the flow of (1). Also, for $S = 0$ and $x > 0$, $S' = DS^0 > 0$, *i.e.*, the vector field points strictly inwards. □

Lemma 2.8. *Solutions of* (1) *are defined and remain bounded for all $t \geq 0$.*

Proof. The proof is identical to the proof of Theorem 4.1 in Section 4 in the case that $n = 1$.

□

Lemma 2.9. *For any $\varepsilon > 0$, there exists $T_\varepsilon \geq 0$ such that $S(t) \leq S^0 + \varepsilon$ for all $t \geq T_\varepsilon$. If in addition, $\lambda < S^0$, $g(S) > D_1$ for $S \in (\lambda, S^0]$, and $x(0) > 0$, then there exists T such that $S(t) < S^0$ for all $t > T$.*

Proof. First suppose that $x(0) = 0$. Then, clearly $S(t)$ converges to S^0.

Now assume that $x(0) > 0$. If there exists $T \geq 0$ such that $S(T) = S^0$, then $S'(T) = -u(S(T))x(T) < 0$. This implies that if there exists $\hat{t} \geq 0$ such that $S(\hat{t}) \leq S^0$ then $S(t) < S^0$ for all $t > \hat{t}$. If $S(t) > S^0$ for all $t \geq 0$, then $S'(t) < 0$ for all $t > 0$. Therefore $S(t)$ converges to some $\alpha \geq S^0$. If $\alpha > S^0$, then $S'(t) < (S^0 - \alpha)D < 0$ for all $t > 0$. But this implies that $S(t)$ converges to $-\infty$ as t tends to ∞, a contradiction. Therefore, either $S(t) \leq S^0$ for all sufficiently large t or $S(t)$ converges to S^0 as $t \to 0$.

Now assume that $\lambda < S^0$, $g(S) > D_1$ for $S \in (\lambda, S^0]$, and $x(0) > 0$. Suppose $S(t) > S^0$ for all $t > 0$. Then, by the continuity of $g(S)$, there exists $\Delta > S^0$ such that $g(S) > D_1$ for all $S \in [S^0, \Delta]$ and there exists a $T_\Delta > 0$ such that $S^0 < S(t) < \Delta$ for all $t > T_\Delta$. Define $\bar{g} \equiv \min_{S \in [S^0, \Delta]} g(S)$. Then $\bar{g} > D_1$. But then, since by Lemma 2.7, $x(t) > 0$ for all $t > 0$, $x'(t)/x(t) > (\bar{g} - D_1) > 0$, for all $t > T_\Delta$. Integrating both sides from T_Δ to ∞, it follows that $x(t) \to \infty$. But, by Lemma 2.8, $x(t)$ is bounded, a contradiction. The result follows. □

2.2.2 *Global stability of equilibrium points*

Theorem 2.10. *If $S^0 \leq \lambda$, then the washout equilibrium, E_0, of (1), is globally asymptotically stable.*

Proof. Since the nonnegative cone is invariant and all solutions are bounded, the result follows immediately from a standard phase portrait analysis. □

Theorem 2.11. *If $\lambda < S^0$, $g'(\lambda) > 0$, $g(S^0) > D_1$, $u'(\lambda) > -\frac{u(\lambda)}{S^0 - \lambda}$ and $1 - \frac{u(S)(S^0 - \lambda)}{u(\lambda)(S^0 - S)}$ has exactly one sign change for $S \in (0, S^0)$, then the equilibrium, $E^*_\lambda = (\lambda, x^*_\lambda)$, is globally asymptotically stable with respect to the interior of the positive cone.*

Proof. First, note that since $g(S^0) > D_1$, it follows that $\lambda < S^0 \leq \mu$, and so by Condition 2.1, E^*_μ is not feasible and that by Condition 2.3, E^*_λ is locally asymptotically stable. Also, by Lemma 2.9, without loss of generality, we need only consider $S \in [0, S^0]$.

Consider the following function,

$$V(S,x) = \int_{\lambda}^{S} \frac{(g(\xi) - D_1)(S^0 - \lambda)}{u(\lambda)(S^0 - \xi)}\, d\xi + x - x^*_\lambda \ln\left(\frac{x}{x^*_\lambda}\right), \tag{9}$$

that is defined and continuously differentiable for $S \in (0, S^0)$ and $x > 0$. For brevity of notation, let

$$\Psi(S) = \frac{u(S)}{S^0 - S}. \tag{10}$$

Then, using (10) it follows that

$$\begin{aligned} \dot{V} &= x(g(S) - D_1)\left(1 - \frac{u(S)(S^0 - \lambda)}{u(\lambda)(S^0 - S)}\right) \\ &= x(g(S) - D_1)\left(1 - \frac{\Psi(S)}{\Psi(\lambda)}\right). \end{aligned} \tag{11}$$

Note that $\dot{V} = 0$ if and only if $S = \lambda$ or $x = 0$ or $S = \mu = S^0$. The derivative of Ψ is given by

$$\frac{u'(S)(S^0 - S) + u(S)}{(S^0 - S)^2}.$$

From Condition 2.3 and by the continuity of u', we have that for S close to λ, $u'(S)(S^0 - S) + u(S) > 0$, and thus the function Ψ is increasing. Also, g is monotone increasing for S near λ. Since each term in (11) changes sign at $S = \lambda$, this implies that for S close to λ, $\dot{V} < 0$. In fact, $\dot{V}$ remains negative as long as neither term in (11) changes sign. But this is ruled out by the hypotheses.

Let $\eta = \{(S,x) \in [0, S^0] : \dot{V}(S,x) = 0\}$. Therefore, $\eta = \{(S,x) \in [0, S^0] : x = 0 \text{ or } S = \lambda \text{ or } S = S^0 = \mu\}$. Let $\mathcal{E}$ denote the largest invariant subset of η. Then $\mathcal{E} = \{(S,0), 0 \le S \le S^0\} \cup \{E^*_\lambda\}$. As solutions are bounded, $\mathcal{E}$ attracts all solutions with nonnegative initial conditions (by the modified LaSalle's Extension Theorem, as stated in [**45,** Th. 1.2]). Noting that from our hypotheses, E_0 is unstable and $E^*_\lambda = (\lambda, x^*_\lambda)$ is locally asymptotically stable, using a standard argument involving the Butler-McGehee Lemma (see [**41**]), it follows that no points of the form $(S,0), S \ge 0$ can be in the omega limit set of any solution initiating inside the positive cone and so the result follows. □

3 Discussion of the yield term There are different mechanisms that lead to the use of a yield term in chemostat models. Consider the following expression relating growth and uptake:

$$g(S) = \rho u(S). \tag{12}$$

As mentioned in the Introduction, one rationale for including the yield term is, historically, to express substrate and organic biomass in the same units. In this case, the yield term is the constant of proportionality in (12).

Another use of the yield coefficient, often confused with the previous one, is to decribe the efficiency of the processes involved. If substrate and microorganism were evaluated in the same units, a perfect reaction would transform one unit of substrate into one unit of microorganism. However, such reactions are not perfect. It is for example possible, in the case of chemical reactions, to compute theoretical yield values from the mass-balance equations of the reactions involved; see, *e.g.*, [**42**]. It is then possible to state that for a given reaction, it takes one mole of reactant to produce ρ moles of product. Equation (12) would in this case give the rate of formation of moles of the new compound as a function of the number of moles of the reactant. Again, in this case ρ would be a constant.

Things are more complicated for more complex processes. In particular, biological processes are prone to a lot of individual variability, making it more difficult to obtain a measure of the efficacy of a biological reaction. Since this measure is very important, for example in the bioprocess field where it serves as an indicator of the economic viability of a given process, the yield has been the object of numerous studies. However, a functional form for the yield has not yet been validated by experiment.

Formally, the yield is the ratio between the amount of matter taken up and the resulting cellular growth, and so it is likely that the yield is not actually constant, but could depend on the substrate concentration, the microbial concentration, and environmental conditions among other things.

In the model studied by Crooke and Tanner [**11**] and Agrawal, Lee, and Ramkrishna [**2**], they assumed that the yield is a function of the substrate concentration, $Y(S)$. They considered monotone growth $g(S)$ and modeled the uptake in system (1) by $u(S) = g(S)/Y(S)$, where $Y(S) = a + bS$. They let

$$\text{(I)} \quad g(S) = \frac{\mu_m S}{K_m + S}, \text{ and so } u(S) = \frac{\mu_m S}{(a + bS)(K_m + S)}, \text{ or}$$

(II) $g(S) = kSe^{(-\frac{S}{K})}$, and so $u(S) = \dfrac{kSe^{(-\frac{S}{K})}}{(a+bS)}$.

Pilyugin and Waltman [**37**] proved that only super-critical Hopf bifurcations are possible in case (I). However, if $Y(S) = a + bS^2$, they proved that both super- and sub-critical Hopf bifurcations are possible.

In the case of constant yield, including the yield term in the substrate equation is mathematically equivalent to including the reciprocal in the microorganism equation instead. One of the important differences in the case that the yield is not constant is that the variable yield term can lead to uptake and growth terms that have different monotonicity properties. Therefore, careful attention to the interpretation of the yield term resulting in its correct placement in the equations is necessary. This is especially true, since the explicit form of the yield function is not yet known. Thus, it is currently only possible to represent the yield in the model using a function that we suspect has similar qualitative properties, e.g., similar monotonicity properties.

If it is assumed that the yield is constant, but that cells need some maintenance energy, then in [**24**], the yield is given by :

$$-\frac{dS}{dt} = \frac{1}{Y}\frac{dx}{dt} + Rx,$$

where R can be interpreted, for example, as the portion of nutrient used for respiration. An alternative approach to modeling the maintenance energy is to consider the yield as a function of the substrate concentration.

Modeling the yield as a function of substrate concentration could also provide an indirect way of modeling storage of nutrient. As well, Godin, Cooper, Rey [**18**] provide experimental evidence that indicates that critical division mass increases as substrate concentration increases and so reproduction rate depends on substrate concentration.

The different interpretations of yield can lead to different forms for the yield functions and different ways to include the yield terms.

4 The general competition model We consider the more general case of several species competing for a common resource using the framework of the previous sections. Here, $x_i(t)$ denotes the concentra-

tion of the ith population of microorganisms at time t.

$$\frac{dS}{dt} = D(S^0 - S) - \sum_{i=1}^{n} x_i u_i(S), \tag{13a}$$

$$\frac{dx_i}{dt} = x_i \left(g_i(S) - D_i\right), \quad i = 1, \ldots, n, \tag{13b}$$

$$S(0) \geq 0, \quad x_i(0) \geq 0, \quad i = 1, \ldots, n.$$

For each species, we define the break-even concentrations λ_i and μ_i as in Section 2. In the case of constant yield, i.e. $u_i(S)$ is proportional to $g_i(S)$ for each $i = 1, 2, \ldots, n$, if the species specific death rates are assumed to be insignificant compared to the dilution rate (i.e. $D_i = D$ for all i or at least D_i sufficiently close to D for all i), the dynamics are well understood. See for example, [**9, 41, 46**]. With constant yield and monotone or inhibitory growth, the competitive exclusion principle holds. At most one species avoids extinction, and its concentration rapidly approaches an equilibrium concentration. In the case of monotone response functions, the species that survives is the one with the lowest break-even concentration. Similar results hold in the case that D_i may not equal D, see for example, [**23, 30, 45, 46**], although this case is not yet completely understood. However, in the case of constant yield, numerical simulations of model (13) to date have only displayed competitive exclusion with convergence to an equilibrium with at most one surviving species.

In the rest of this paper, we demonstrate that in the case of variable yield, more exotic dynamical behavior seems to be possible.

Before we consider specific examples we make the following observations.

Theorem 4.1. *Both the nonnegative cone and the interior of the nonnegative cone are invariant under the flow of* (13) *and all solutions are defined and remain bounded for all* $t \geq 0$.

Proof. An argument similar to that given to prove Lemma 2.7 can be used to establish that solutions are nonnegative and hence bounded below, so it remains only to prove that all solutions are bounded above.

Without loss of generality, assume that $x_i(0) > 0$ and thus $x_i(t) > 0$ for all $i \in \{1, ..., n\}$ and all $t \geq 0$ in the domain of definition of the solution $(S(t), x_1(t), ..., x_n(t))$. Let $\hat{S} = \max(S(0), S^0)$. Then the nonnegativity of solutions implies that $S(t) \leq \widehat{S}$ for all $t \geq 0$ for which

$S(t)$ is defined. Since $g_i(0) = 0$, by the continuity of g_i, there exists $\varepsilon > 0$ such that $g_i(S) \le D_i/2$ for all $0 \le S \le \varepsilon$ and all $i \in \{1, ..., n\}$. In addition, there exists $M_\varepsilon > 0$ such that

$$\frac{g_i(S) - D_i + D}{u_i(S)} \le M_\varepsilon, \quad \forall S \in [\varepsilon, \widehat{S}],\ \forall i \in \{1, ..., n\}.$$

Let $\hat{x} > M_\varepsilon(\widehat{S} - \varepsilon)$ and define $\widehat{\Omega}(\hat{x})$ to be the set

$$\widehat{\Omega}(\hat{x}) = \Big\{(S, x_1, ..., x_n) \subset \mathbb{R}_+^{n+1} :\ S \le \widehat{S},\ \sum_{i=1}^n x_i \le \min(\hat{x}, \hat{x} - M_\varepsilon(S - \varepsilon))\Big\}.$$

Choose $\hat{x}$ sufficiently large so that $(S(0), x_1(0), ..., x_n(0)) \in \widehat{\Omega}(\hat{x})$.

We have already established that $0 \le S(t) \le \widehat{S}$. If $(S, x_1, ..., x_n)$ is a point on the relevant part of the boundary of $\widehat{\Omega}(\hat{x})$, then either $S < \varepsilon$ and $\sum_{i=1}^n x_i = \hat{x}$, or $\varepsilon \le S \le \hat{S}$ and $\sum_{i=1}^n x_i = \hat{x} - M_\varepsilon(S - \varepsilon)$. In the former case, we have that

$$\Big(\sum_{i=1}^n x_i\Big)' = \sum_{i=1}^n x_i(g_i(S) - D_i) \le -\sum_{i=1}^n \frac{x_i D_i}{2} < 0,$$

since we assumed $x_i > 0$. In the latter case, we have that

$$\Big(S + \sum_{i=1}^n \frac{x_i}{M_\varepsilon}\Big)' = D\Big(S^0 - S - \sum_{i=1}^n \frac{x_i}{M_\varepsilon}\Big) + \sum_{i=1}^n \frac{x_i}{M_\varepsilon}\big(-M_\varepsilon u_i(S) + (g_i(S) - D_i + D)\big).$$

Since $\varepsilon \le S \le \widehat{S}$, the choice of M_ε warrants that

$$\sum_{i=1}^n \frac{x_i}{M_\varepsilon}\big(-M_\varepsilon u_i(S) + (g_i(S) - D_i + D)\big) \le 0.$$

Consequently,

$$\Big(S + \sum_{i=1}^n \frac{x_i}{M_\varepsilon}\Big)' \le D\Big(S^0 - S - \sum_{i=1}^n \frac{x_i}{M_\varepsilon}\Big) = D\Big(S^0 - \varepsilon - \frac{\hat{x}}{M_\varepsilon}\Big) < 0,$$

because $S^0 \leq \widehat{S} < \varepsilon + (\hat{x}/M_\varepsilon)$ by the choice of $\hat{x}$. We conclude that the vector field of (13) points strictly into the interior of $\widehat{\Omega}(\hat{x})$ when restricted to the part of the boundary $\partial\widehat{\Omega}$ with $x_i > 0,\ i = 1, 2, \ldots, n$ and $0 \leq S \leq \widehat{S}$. Also, since $x_i(0) > 0$, we have that $x_i(t) > 0$, for all $i = 1, \ldots, n$, and $t > 0$. Thus $(S(t), x_1(t), ..., x_n(t)) \in \widehat{\Omega}(\hat{x})$ for all $t \geq 0$. Since $\widehat{\Omega}$ is bounded, $(S(t), x_1(t), ..., x_n(t))$ must be bounded for all $t \geq 0$. □

Lemma 4.2. *In* (13)*, if for some* $i \in \{1, \ldots, n\}$*,* $\lambda_i > S^0$*, then* $x_i(t) \to 0$ *as* $t \to \infty$*.*

Proof. Using an argument similar to that given to prove Lemma 2.9, it follows that there exists $\epsilon > 0$, and $T > 0$ such that $S(t) < S^0 + \epsilon < \lambda_i$, for all $t \geq T$. By Lemma 4.1 $x_i(t)$ is nonnegative, and so $x_i'(t)/x_i(t) < -D_i + g_i(S^0 + \epsilon) < 0 = -D_i + g_i(\lambda_i)$, for all $t > T$. Integrating from $t = T$ to ∞, it follows that $x_i(t) \to 0$ as $t \to \infty$. □

The next two results are helpful for constructing examples in which coexistence is possible.

Theorem 4.3. *Suppose that*

(i) *there exist nonempty sets* $I_-, I_+ \subset \{1, ..., n\}$ *and* $\alpha_i > 0$ *such that* $I_- \bigcap I_+ = \varnothing$ *and*

$$G(S) = \sum_{i \in I_-} \alpha_i (g_i(S) - D_i) - \sum_{i \in I_+} \alpha_i (g_i(S) - D_i) < 0 \tag{14}$$

$$\text{for all } \ S \in (0, S^0);$$

(ii) *there exists* $j \in I_+$ *such that* $g_j(S^0) > D_j$*.*

Then for any positive solution $(S(t), x_1(t), ..., x_n(t))$ *of* (13)*,*

$$\lim_{t \to \infty} \prod_{i \in I_-} x_i^{\alpha_i}(t) = 0.$$

Proof. By Theorem 4.1, there exists $M > 0$ such that $0 \leq x_i(t) \leq M$ for all $i = 1, ..., n$ and $t \geq 0$. Equation (13a) then implies that there exists a sufficiently small $\delta > 0$ such that $S(t) \geq \delta$ for all sufficiently large t. By an argument similar to that given in Lemma 2.9, $S(t) < S^0$

for all sufficiently large t. Therefore, there exists $T > 0$ such that $0 < \delta < S(t) < S^0$ for all $t > T$.

For all $i \in I_- \cup I_+$, define $z_i(t) = x_i^{\alpha_i}(t)$. Then

$$z_i'(t) = \alpha_i x_i^{\alpha_i - 1}(t)\ x_i(t)(g_i(S(t)) - D_i) = z_i(t)\ \alpha_i(g_i(S(t)) - D_i).$$

Let

$$\xi(t) = \frac{\prod_{i \in I_-} z_i(t)}{\prod_{i \in I_+} z_i(t)}.$$

Then

$$\xi'(t) = \xi(t) G(S(t)).$$

Since $S(t) \in [\delta, S^0)$ for all $t > T$, $G(S(t)) < 0$ so that $\xi(t)$ is a strictly decreasing function for $t > T$ bounded below by 0. It follows that there exists $\xi_0 = \lim_{t \to \infty} \xi(t) \geq 0$. Now there are two possibilities. The first possibility is that $\xi_0 = 0$ in which case

$$0 \leq \lim_{t \to \infty} \prod_{i \in I_-} z_i(t) \leq \left(\prod_{i \in I_+} M^{\alpha_i} \right) \lim_{t \to \infty} \xi(t) = 0.$$

The second possibility is that $\xi_0 > 0$, in which case, a theorem by Hadamard and Littlewood [**32**] implies that $\lim_{t \to \infty} G(S(t)) = 0$. Since $S(t) \in [\delta, S^0)$ for all $t > T$, it must be the case that $\lim_{t \to \infty} S(t) = S^0$. But this conclusion would contradict the boundedness of $x_j(t)$ and hence the assertion $\xi_0 > 0$ is invalid. The result follows by observing that

$$\lim_{t \to \infty} \prod_{i \in I_-} x_i^{\alpha_i}(t) = \lim_{t \to \infty} \prod_{i \in I_-} z_i(t) = 0.$$

□

Corollary 4.4. *If the set I_- is a singleton, that is, $I_- = \{i^*\}$, then the assumptions* (i) *and* (ii) *imply that for any positive solution $(S(t), x_1(t), ..., x_n(t))$ of* (13)*,*

$$\lim_{t \to \infty} x_{i^*}(t) = 0.$$

In the population dynamics literature, two types of coexistence are distinguished: strong and weak. We say that a positive solution $(S(t), x_1(t), ..., x_n(t))$ exhibits strong coexistence if $\liminf_{t \to \infty} x_i(t) > 0$,

for all $i \in \{1, ..., n\}$ and it exhibits weak coexistence if $\limsup_{t\to\infty} x_i(t) > 0$, for all $i \in \{1, ..., n\}$. Using this terminology, Theorem 4.3 provides a necessary condition for strong coexistence. The conclusion that

$$\lim_{t\to\infty} \prod_{i\in I_-} x_i^{\alpha_i}(t) = 0$$

is insufficient to eliminate the possibility of weak coexistence. We would like to point out that Rao and Roxin [**40**] have obtained an equivalent criterion for strong coexistence using the methods of control theory for constant yields ($g_i(S) = k_i u_i(S)$) and a time dependent input feed concentration ($S^0 = S^0(t)$).

4.1 Yield included in the uptake equation Here, we consider model (13) of the chemostat in which two microbial species $x_1 = x$ and $x_2 = y$ compete for a single substrate S. We assume that the species x has a variable yield while the species y has a constant yield. As we pointed out previously, there are two ways to incorporate the variable yield into the model. In this section we choose to incorporate the yield into the consumption (uptake) rate of species x. In addition, we assume that the variables x, y, and S, and time t, have been rescaled appropriately so that both the dilution rate D and the substrate feed concentration S^0 equal unity, that is, $D = S^0 = 1$. The model then takes the form

$$\frac{dS}{dt} = 1 - S - x\,\frac{p_1(S)}{\gamma_1(S)} - y\,\frac{p_2(S)}{\gamma_2}, \tag{15a}$$

$$\frac{dx}{dt} = x(p_1(S) - 1), \tag{15b}$$

$$\frac{dy}{dt} = y(p_2(S) - 1), \tag{15c}$$

$$S(0) \geq 0, \quad x(0) \geq 0, \quad y(0) \geq 0.$$

We assume that the specific growth rates $p_1(S)$ and $p_2(S)$ are expressed in the traditional Monod formulation

$$p_i(S) = \frac{m_i S}{a_i + S}, \quad i = 1, 2,$$

and the variable yield coefficient of the species x is given by $\gamma_1(S) = b_1 + c_1 S^n$ where $b_1, c_1 > 0$ and n is a positive integer. For a more detailed description of the model (15) we refer the reader to [**37**].

For reasons that will be explained below, we choose to treat c_1 and m_2 as bifurcation parameters. The rest of the parameters will be fixed as shown in Table 1.

TABLE 1: Parameter values for model (15).

$m_1 = 2.0$	m_2 varies
$a_1 = 0.7$	$a_2 = 6.5$
$b_1 = 1.0$	$\gamma_2 = 120.0$
c_1 varies	$n = 4$

The break-even concentrations λ_i of the species x and y can be obtained by solving $p_i(\lambda_i) = 1$:

$$\lambda_1 = \frac{a_1}{m_1 - 1} = 0.7, \qquad \lambda_2 = \frac{a_2}{m_2 - 1}.$$

Since $\lambda_1 < 1$, species x will persist in the absence of species y. A necessary condition for the species y to persist in the culture is that $\lambda_2 < 1$, or equivalently, $m_2 > 7.5$.

Corollary 4.4 implies that a necessary condition for coexistence is that the graphs of $p_1(S)$ and $p_2(S)$ intersect at some point $0 < \widehat{S} < 1$. In model (15),

$$\widehat{S} = \frac{m_1 a_2 - m_2 a_1}{m_2 - m_1}$$

so that a necessary condition for coexistence is

$$8.82 = m_1 \frac{a_2}{a_1} < m_2 < m_1 \frac{a_2 + 1}{a_1 + 1} = 18.57.$$

If $m_2 < 8.82$, then x will always drive y to extinction. If $m_2 > 18.57$, then y will always drive x to extinction. Both of these conclusions hold regardless of any particular dynamic behavior of the full system (e.g., equilibrium, periodic solution, or other) and specifically they are independent of the functional form of the variable yield coefficient $\gamma_1(S)$. If $\gamma_1(S) = \gamma_1$ were constant, then the outcome of competition would be completely determined by the inequality $\lambda_1 < \lambda_2$ and whether or not $\lambda < 1$. The critical value of m_2 for which $\lambda_1 = \lambda_2$ is given by $m_2 = 1 + (m_1 - 1)(a_2/a_1) = 10.286$.

4.1.1 *Bifurcation to coexistence* The fact that single species continuous cultures with variable yields may exhibit sustained oscillations has an important implication for coexistence. The principle of competitive exclusion states that two species cannot coexist *at equilibrium* when they compete for a single substrate in continuous culture. The first proof of this assertion was presented in [**23**] for Monod uptake rates and it was later extended to a much broader class of growth rates and uptake functions in [**45**]. In [**8**], a two predator - one prey ecosystem was studied in the chemostat setting. It was shown that such a system may exhibit a stable periodic solution with both competing predators present at all times. Specifically, it was shown that the stable limit cycle corresponding to sustained oscillations of a single predator population can bifurcate into the region of coexistence and preserve its stability. In [**37**], it was demonstrated that the same type of bifurcation can occur in the chemostat when one competitor exhibits a variable yield and the other competitor has a constant yield. If $\Gamma = (S(t), x(t))$ is a stable periodic solution of (15) of period $T > 0$ with $y = 0$, then Γ undergoes a transcritical bifurcation when m_2 increases past the bifurcation value

$$m_2^* = \frac{T}{\int_0^T \frac{S(t)}{a_2+S(t)}\,dt}. \tag{16}$$

The stable periodic solution of (15) with $x(t), y(t) > 0$ exists for $m_2 > m_2^*$.

If we let $y = 0$ in (15) then the reduced model (15a–15b) undergoes a Hopf bifurcation when c_1 crosses the value

$$\hat{c}_1 = \frac{(m_1-1)^4\big((m_1-1)^2 + a_1\big)}{a_1^4(3m_1^2 - 4m_1a_1 - 2m_1 - a_1 - 1)}. \tag{17}$$

For the parameter values given in Table 1, the Hopf bifurcation occurs at $\hat{c}_1 = 10.115$. Furthermore, the Hopf bifurcation is *supercritical* for $m_2 = 2,\ a_2 = 0.7,\ n = 4$, that is, the stable limit cycle of (15a–15b) exists for $c_1 > \hat{c}_1$.

To compute the bifurcation value m_2^* for different values of c_1, we implemented the formula (16) as follows. If $c_1 < \hat{c}_1$ and the stable limit cycle of (15a–15b) does not exist, then we let

$$m_2^* = \frac{a_2 + \lambda_1}{\lambda_1},$$

which is the limiting case of (16) as $S(t) \to \lambda_1$ and $T \to \infty$. If $c_1 > \hat{c}_1$, then the stable limit cycle Γ does exist and we first integrate (15a–15b)

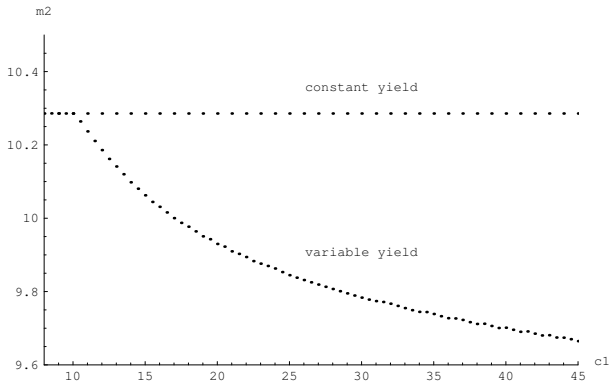

FIGURE 2: A transcritical bifurcation to coexistence for a given value of c_1 occurs at m_2^* given by the lower curve on the graph. The straight line shows the value $m_2 = 10.286$ at which the break-even concentrations are equal ($\lambda_1 = \lambda_2 = 0.7$). The transcritical bifurcation occurs only in the region $c_1 > \hat{c}_1 = 10.115$ where the reduced system (15a–15b) with $y = 0$ exhibits a stable limit cycle. If c_1 is fixed and m_2 crosses the bifurcation value m_2^*, the stable limit cycle bifurcates into the coexistence region $x, y > 0$.

with $y = 0$ in forward time to approximate Γ and then use (16) to find m_2^*. The output of this numerical procedure is shown in Figure 2.

In the remainder of this section, we present a numerical study of the dynamics exhibited by solutions which correspond to competitive coexistence in the case $\lambda_1 < \lambda_2 < 1$, $c > \hat{c}$ and $m_2 > m_2^*$. Considering the dynamics on the invariant planes $F_x = \{S, x \geq 0,\ y = 0\}$ and $F_y = \{x = 0,\ S, y \geq 0\}$, this is the case when almost all positive solutions correspond to coexistence, that is,

$$\limsup_{t\to\infty} x(t) > 0, \quad \limsup_{t\to\infty} y(t) > 0.$$

To see this, let $W^s(E)$ and $W^u(E)$ denote the stable and unstable manifold of the equilibrium E, respectively. Observe that both F_x and F_y contain the (trivial) equilibrium $E_0 = (1, 0, 0)$ which is a saddle with $\dim W^u(E_0) = 2$. In addition, F_x contains the equilibrium $E_1 = (\lambda_1, x^*, 0)$ and F_y contains the equilibrium $E_2 = (\lambda_2, 0, y^*)$. Since y has a constant yield, E_2 is a local attractor relative to F_y, that is, $\dim W^s(E_2) = 2$ with $W^s(E_2) \subset F_y$ and the inequality $\lambda_1 < \lambda_2$ guarantees that $\dim W^u(E_2) = 1$ with $W^u(E_1) \subset \mathbb{R}^3_+$. Thus, E_1 repels towards

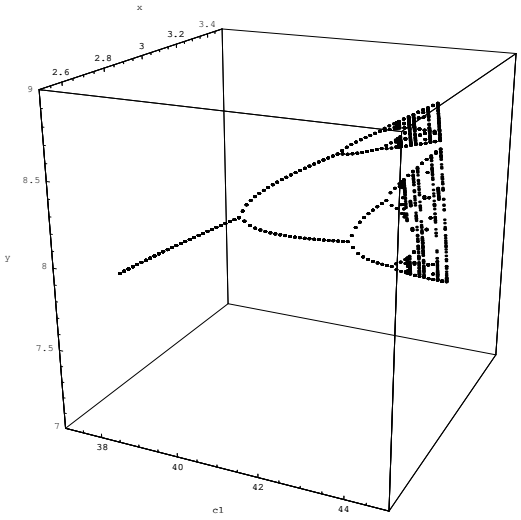

FIGURE 3: A cascade of period-doubling bifurcations leading to a chaotic attractor shown here with $m_2 = 10.0$.

the interior of $\mathbb{R}^3_+$. If $c > \hat{c}$, then $\dim W^u(E_1) = 2$ with $W^u(E_1) \subset F_x$ and $\dim W^s(E_1) = 1$ with $W^s(E_1) \subset \mathbb{R}^3_+$. Furthermore, since $c > \hat{c}$ and $m_2 > m_2^*$, there exists an unstable limit cycle Γ sitting in F_x that is a saddle with respect to $\mathbb{R}^3$. It is attracting in F_x, but repels into the interior of $\mathbb{R}^3$ and $\dim W^s(\Gamma) = 2$, $\dim W^u(\Gamma) = 2$, and $W^u(\Gamma) \cap \mathbb{R}^3_+ \neq \varnothing$ so that Γ repels towards the interior of $\mathbb{R}^3_+$. Using the Butler-McGehee lemma, we conclude that no solution except those on $W^s(E_1)$ can have their ω-limit sets contained entirely in F_x or F_y. Consequently, almost all positive solutions correspond to coexistence.

4.1.2 *Period-doubling cascade leads to chaos* The proven tool for studying periodic solutions is the Poincaré map. We observe that any positive solution of (15) that corresponds to coexistence must have the property that $S(t)$ attains the values $S = \lambda_1$ and $S = \lambda_2$ infinitely often with the signs of S' alternating. Therefore, it is natural to study the Poincaré map defined on one of these surfaces. Since we decided to fix m_1 and a_1, it is appropriate to consider the Poincaré map P on $S = \lambda_1 = 0.7$. For convenience, we define the Poincaré map to be the second return map so that the sign of S' is the same for all consecutive intersections.

Our first finding is that the periodic solution that bifurcates into

the positive cone giving coexistence can undergo a cascade of period-doubling bifurcations ultimately resulting in a chaotic attractor. The bifurcation diagram illustrating the period-doubling cascade is shown in Figure 3. Figure 4(a) shows the forward trajectory approximating the attractor and Figure 4(b), the cross-section of the attractor with $m_2 = 10.0,\ c_1 = 45.0$. Numerically, we computed the cross-section by constructing a sequence $\{(x_n, y_n)|n = 1, ..., N\}$ $(N = 5000)$ with

$$(x_{n+1}, y_{n+1}) = P(x_n, y_n)$$

by performing a different forward integration for each n to avoid error accumulation for long trajectories.

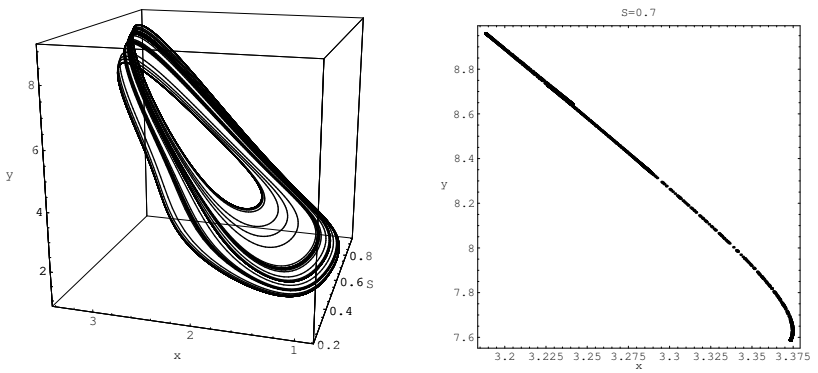

(a) (b)

FIGURE 4: (a) Chaotic attractor corresponding to $m_2 = 10.0,\ c_1 = 45.0$. (b) The cross-section $S = \lambda_1$ of the attractor.

4.1.3 *A nontrivial periodic trajectory* A natural consequence of a period-doubling cascade is the existence of periodic trajectories of arbitrarily large periods. In addition to these, we have found periodic trajectories that have a rather peculiar geometry. We present a numerical example of such a trajectory in Figure 5(a). We speculate that this trajectory switches between the domains of influence of $W^s(E_1)$ (when it spirals

towards the lower values of y) for small amplitudes and of $W^u(\Gamma)$ (when it spirals towards the higher values of y) for large amplitudes.

We obtained the periodic trajectory shown in Figure 5(a) by integration in forward time and then determined the period by minimizing the distance between the initial point $(S(0), x(0), y(0))$ and $(S(T), x(T), y(T))$ so that

$$T = \arg\min_T \sqrt{(S(T) - S(0))^2 + (x(T) - x(0))^2 + (y(T) - y(0))^2}.$$

If we write (13) using vector notation $z = (S, x, y)$ as $\dot{z} = F(z)$, the variational system of (13) along the periodic solution $z(t) = (S(t), x(t), y(t))$ is expressed as $\dot{\phi}(t) = \partial F/\partial z(z(t))\phi(t)$. After obtaining an estimate of the period T, we numerically integrated the initial value problem

$$\dot{X}(t) = \frac{\partial F}{\partial z}(z(t))X(t), \quad X(0) = I,$$

where I is the 3×3 identity matrix, from $t = 0$ to $t = T$. Then we estimated the Floquet multipliers of the periodic solution $z(t) = (S(t), x(t), y(t))$ as the eigenvalues of $X(T)$.

The estimates of Floquet multipliers are

$$\mu_1 = 1.0008, \quad \mu_2 = 0.827, \quad \mu_3 = 6.73 \cdot 10^{-6}.$$

Of course, the actual value of the first multiplier should be $\mu_1 = 1$. But the fact that $\mu_2,\ \mu_3 < 1$ supports the evidence that this periodic solution is stable.

4.1.4 *Existence of linked attractors* Here, we present the case $c_1 = 38.3,\ m_2 = 10.1$ where we found two stable periodic trajectories shown in Figure 5(b). The most interesting feature of these trajectories is that they are topologically linked. The first trajectory (thick line) has the period $T_1 = 17.055$ and the second trajectory (thin line) has the period $T_2 = 98.933$. The linking exists because the second trajectory passes inside of the thick loop on its way "down" and outside of the loop on its way "up". Both periodic trajectories were obtained by forward integration.

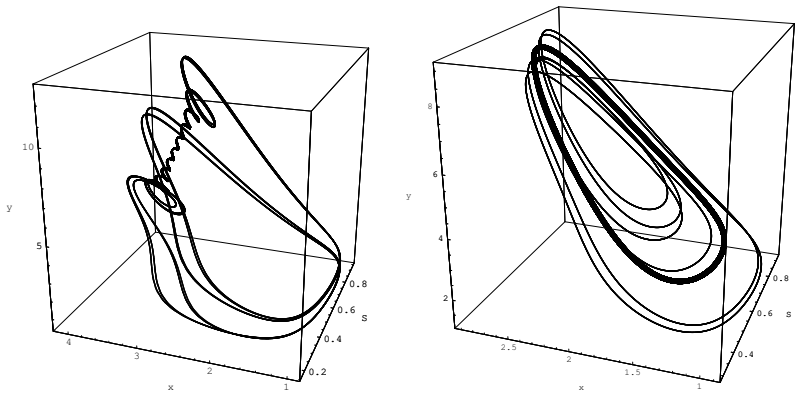

(a) (b)

FIGURE 5: (a) A periodic solution of period $T = 672.713$ for $c_1 = 55.0$ and $m_2 = 10.1809$ with initial conditions $S(0) = 0.711,\ x(0) = 3.199,\ y(0) = 9.779$. The numerical values of Floquet multipliers are $\mu_1 = 1.0008,\ \mu_2 = 0.827,\ \mu_3 = 6.73{\cdot}10^{-6}$. Of course, the true value of μ_1 must be unity. Since $|\mu_2|,\ |\mu_3| < 1$, we believe that this solution is stable. (b) Two stable periodic trajectories shown here for $c_1 = 38.3,\ m_2 = 10.1$ are topologically linked. The first trajectory (thick line) has the period $T_1 = 17.055$ and initial conditions $S(0) = 0.547,\ x(0) = 1.282,\ y(0) = 2.227$. The second trajectory (thin line) has the period $T_2 = 98.933$ and initial conditions $S(0) = 0.808,\ x(0) = 1.823,\ y(0) = 4.033$.

4.1.5 *Neimark-Sacker bifurcation* In a Neimark-Sacker bifurcation, both eigenvalues of the Poincaré map cross the unit circle. The periodic orbit persists but changes its stability. The stable limit cycle is replaced by a stable invariant torus that may have either rational or irrational rotation number. In either case, the species still coexist although the corresponding orbit may no longer be periodic. Specifically, in case of an irrational rotation number, such an orbit will be dense on the invariant torus produced via the Neimark-Sacker bifurcation. Figure 6(a) is a bifurcation diagram that shows one instance of the (supercritical) Neimark-Sacker bifurcation. This diagram was computed with $c_1 = 37.0$, and it shows quite nicely how the stable periodic orbit is replaced by an invariant torus, and then the torus itself is replaced by a more complicated strange

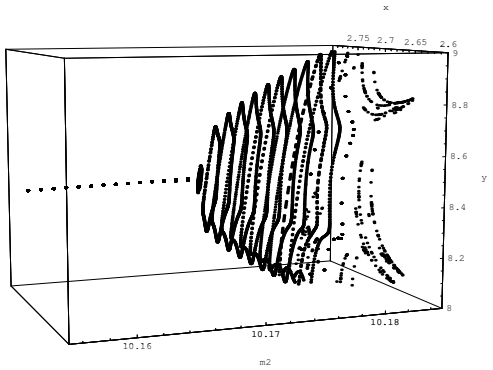

(a)

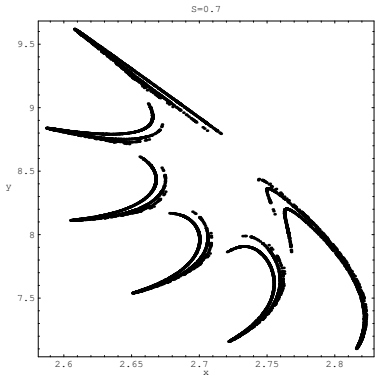

(b)

FIGURE 6: (a) The bifurcation diagram for $c_1 = 37.0$. Here m_2 is the bifurcation parameter. (b) The cross-section of the strange attractor with $c_1 = 37.0, m_2 = 10.181$.

attractor. Figure 6(b) shows a cross section of the strange attractor when the invariant torus loses its smoothness and breaks up.

4.2 Yield included in the growth equation In the following, we specialize system (13) to the case of three competing species and assume

that x_i models the concentration of species i. We assume that $u_i(S)$ models the uptake of nutrient and that the growth term takes the form $g_i(S) = Y_i(S)u_i(S)$. One interpretation of the yield $Y_i(S)$ in this section is to model the efficacy of the conversion process and allow it to depend on the substrate concentration.

We will study an example in which $Y_1(S)$ depends on substrate concentration, and hence is variable, whereas the $Y_i(S) = Y_i, \quad i = 2, 3$ are constant. Our aim here is not only to show three species coexistence is possible in this setting providing another example that contradicts the *principle of competitive exclusion*, but also to show that competitor-mediated coexistence is possible. In particular, it is possible that all three species can coexist, but that if one of the species is removed, then only one species is able to survive.

Since $Y_i, \ i = 2, 3$ are constant, in the absence of species x_1, under very general assumptions on the form of $u_i(S), \ i = 2, 3$ (see e.g., [**30, 45, 46**]) at most one species can survive and the concentrations of substrate and organisms equilibrate. Thus we will try to show that by introducing population x_1 with a variable yield, we can obtain coexistence of all three populations, and hence competitor-mediated coexistence.

As discussed in the previous subsection, in order to obtain coexistence it is necessary to have oscillatory solutions. By (7), if we restrict ourselves to $(S - x_1)$-space, and assume $x_i(t) \equiv 0, \ i = 2, 3$, then a Hopf bifurcation can only occur at an equilibrium of the form $E^*_{\lambda_1}$ where $g_1'(\lambda_1) > 0$ and $u_1'(\lambda_1) < 0$. Here we also assume that $g_1(S) = Y_1(S)u_1(S)$. Therefore, $u_1(S)$ must be inhibitory at high concentrations, and hence we use unimodal functions to model uptake.

Since the input concentration S^0 is one of the parameters that the experimenter often has control over, in this section we consider S^0 as a bifurcation parameter.

For our purposes, the uptake functions $u_i, \ i = 1, 2, 3$, are taken to be the following one humped functions:

$$u_1(S) = \frac{4S}{0.25S^2 + 0.5S + 0.2},$$
$$u_2(S) = \frac{11S}{S^2 + S + 2},$$
$$u_3(S) = \frac{2.98S}{1.227S^2 + 3.5S + 3.225}.$$

They have the relative forms shown in Figure 7(a).

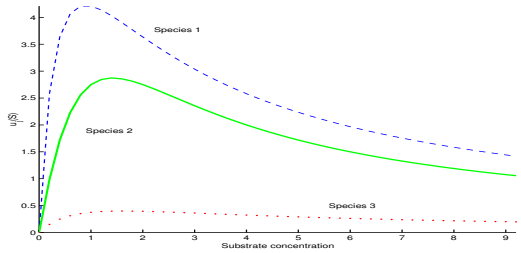

(a)

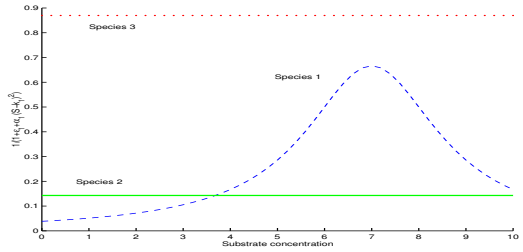

(b)

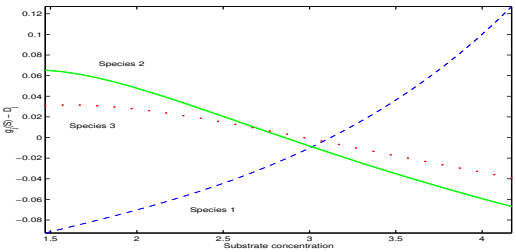

(c)

FIGURE 7: (a) Consumption rates $u_i(S)$, $i = 1, 2, 3$. (b) Yield functions $Y_i(S)$, for $i = 1, 2, 3$. Only species x_1 has a variable yield. All yields are fractions (less than one). (c) Per capita growth rate, $g_i(S) - D_i$ for values of substrate on a coexistence periodic orbit, $1.475 < S < 4.24$, and S^0=9.3.

Since we are interpreting the yield as the efficacy of the conversion process, we expect the yield to be a positive fraction. Since we have not been able to find any experimental support for any particular functional form modeling this efficacy, we assume that it is unimodal, initially increasing. In our example, we take $Y_i(S)$ to have the form:

$$Y_i(S) = \frac{1}{1 + \epsilon_i + \alpha_i(S - k_i)^2}.$$

Since we assume that only species x_1 has a variable yield, this means that $\alpha_2 = \alpha_3 = 0$. We set $\alpha_1 = 0.5$, $\epsilon_1 = 0.5$, $\epsilon_2 = 6$, $\epsilon_3 = 0.15$, and $k_1 = 7$. Figure 7(b) shows the yield functions $Y_i(S)$, for the three species.

The dilution rate is assumed to be $D = 0.31$. We take $D_1 = 0.33$, $D_2 = 0.345, D_3 = 0.315$. Thus the per capita growth rate of the various populations is given by:

$$g_1(S) - D_1 = \frac{u_1(S)}{1 + 0.5 + 0.5(S - 7)^2} - 0.33,$$

$$g_2(S) - D_2 = \frac{u_2(S)}{7} - 0.345,$$

$$g_3(S) - D_3 = \frac{u_3(S)}{1.15} - 0.315.$$

The graphs of these functions, demonstrating how they intersect, are shown in Figure 7(c). Here, S is in the range $1.475 < S < 4.24$. This corresponds to values on a periodic orbit in which all three species coexist, shown later in this section (see Figure 10(d)). It is clear that each population has an advantage over both of its competitors at some concentrations of the substrate and that the hypotheses of Theorem 4.3 and Corollary 4.4 are not satisfied.

Recall that by definition the break-even concentrations λ_i and μ_i are the solutions of $g_i(S) - D_i = 0$. For the parameters that we have selected,

$$\lambda_1 = 3.1239, \qquad \mu_1 = 9.3421;$$
$$\lambda_2 = 0.7007, \qquad \mu_2 = 2.8541;$$
$$\lambda_3 = 0.8865, \qquad \mu_3 = 2.9657.$$

Hence, if we were in the case of constant yield, based on the relative values of these break-even concentrations, if $S^0 > \lambda_2$, we would conclude that species x_3 would be driven to extinction, if $x_2(0) > 0$. Whether population x_1 or x_2 would win the competition or whether both populations would wash out of the chemostat would depend on the initial conditions and the concentration of S^0.

To obtain coexistence of all three species, it is important that the substrate concentration oscillates between values where each of the species has an advantage. The "trick" to obtain coexistence in the variable yield model is to set things up so that as the bifurcation parameter S^0 varies, there is a Hopf bifurcation in the $(S - x_1)$ plane, followed by a transcritical bifurcation of limit cycles, resulting in a periodic orbit with two species coexisting, and finally another transcritical bifurcation of limit cycles involving all three species. Of course, to claim coexistence, the resulting limit cycle involving all three species must be orbitally asymptotically stable in some open set of parameter space.

We illustrate this in the following sequence of bifurcation diagrams and numerical simulations. We use the XPPAUT interface to Auto (see [**5**]) to produce the bifurcation diagrams shown in Figures 8(a), 9(a)-9(c) and 10(a)-10(c). In these figures solid lines indicate asymptotically stable equilibria, dashed lines, indicate unstable equilibria, filled in dots indicate orbitally asymptotically stable periodic orbits, and open dots indicate unstable periodic orbits. For periodic orbits, we use the "Hi-Lo feature", *i*.e. for each value of the bifurcation parameter S^0, the largest and smallest value of the coordinate labeled on the ordinate axis is graphed.

First we restrict our attention to the $(S - x_1)$-face. Figure 8(a) shows two bifurcations with the stability with respect to this face only. An analogous bifurcation diagram is shown in Figure 9(a) with the stability given with respect to $(S, x_1, x_2, x_3)-$space. This diagram was plotted with XPPAUT, and shows the minimal and maximal value of x_1, along the periodic orbit, for different values of S^0. There is a subcritical Hopf bifurcation at $S^0 = 8.984$, and a saddle node of limit cycles at $S^0 = 8.833$. Figure 8(b), shows two periodic orbits in the (S, x_1)-face, for $S^0 = 8.92$. There are two periodic orbits. The inner orbit is unstable and the outer one is asymptotically stable. The unstable orbit was plotted using reversed time integration.

Figure 9 shows bifurcation curves for which x_1 and x_2 are nonnegative, but $x_3 = 0$. In this figure the stability is given with respect to (S, x_1, x_2, x_3)-space. Comparing Figure 8(a) with Figure 9(a), we see that besides the Hopf bifurcation and the saddle node of limit cycles

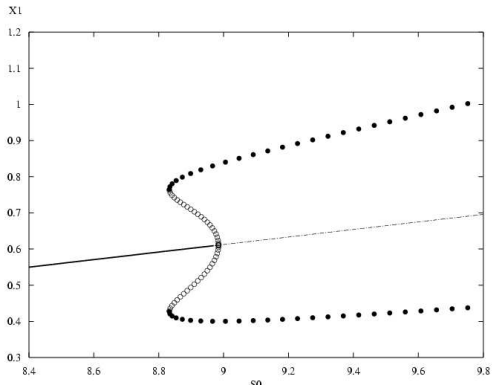

(a)

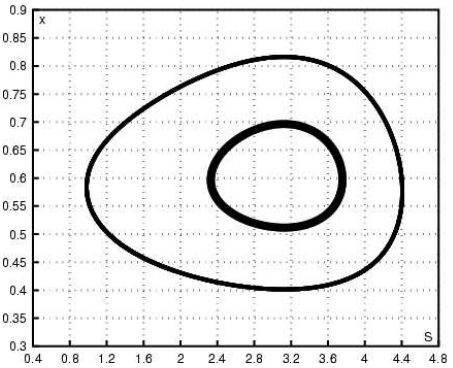

(b)

FIGURE 8: (a) Bifurcation diagram with stability with respect to $(S - x_1)$-space only. This figure shows two bifurcations: at $S^0 = 8.984$, there is a subcritical Hopf bifurcation; at $S^0 = 8.833$, a saddle node of limit cycles. (b) Numerical simulation showing two periodic orbits in the $(S - x_1)$-face when $S^0 = 8.92$, as predicted by the bifurcation diagram. The inside one is unstable and the outside one is orbitally asymptotically stable.

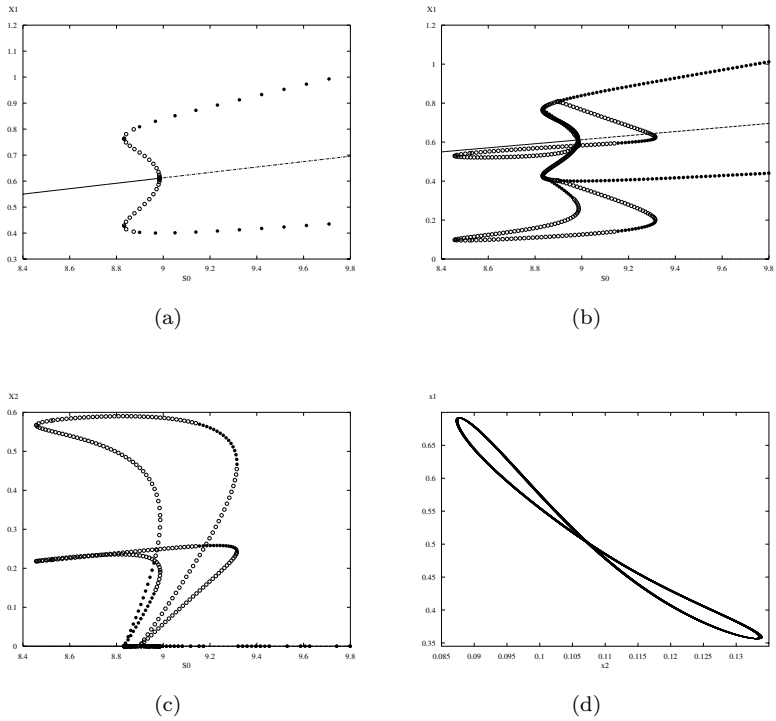

FIGURE 9: (a)–(c) Bifurcation diagrams showing stability with respect to (S, x_1, x_2, x_3)-space. (a) Bifurcations in the (S, x_1)-face. Besides the Hopf and saddle node bifurcations shown in Figure 8(a), there is a branch point at $S^0 = 8.899$. Only bifurcations with $x_1 > 0$ and $x_i = 0,\ i = 2, 3$ are shown. (b) and (c) Only bifurcation curves with species x_1 and x_2 nonnegative and $x_3 = 0$ are shown. There is stable coexistence of species x_1 and x_2 for $8.833 < S^0 < 8.968$ and $9.155 < S^0 < 9.315$. (d) A numerical simulation showing stable oscillatory coexistence of x_1 and x_2, for $S^0 = 8.92$.

in the (S, x_1)-face, there is a branch point at $S^0 = 8.899$. The outer periodic orbit that is stable with respect to (S, x_1)-space is unstable for $8.833 < S^0 < 8.899$ with respect to (S, x_1, x_2, x_3)-space. There is a transcritical bifurcation of limit cycles as S^0 increases through the branch point $S^0 = 8.899$, resulting in a branch of unstable periodic orbits with

$x_i > 0,\ i = 1, 2$. Along this branch, when S^0 increases through 9.315 this branch stabilizes and the periodic orbits remain stable until S^0 decreases through 9.155. Hence, there is stable coexistence of species x_1 and x_2 for $9.155 < S^0 < 9.315$. Continuing along this branch, it stabilizes again as S^0 decreases through 8.968 and remains stable until it collapses into the plane via a transcritical bifurcation at approximately 8.833. So there is also stable coexistence of x_1 and x_2 for $8.833 < S^0 < 8.968$. An example of this oscillatory coexistence of x_1 and x_2 is shown shown in Figure 9(d).

Figure 10 shows bifurcation curves for which $x_i \geq 0,\ i = 1, 2, 3$. There is a transcritical bifurcation of the limit cycle in the (S, x_1, x_2)-face (with $x_3 \equiv 0$) into the positive cone. This branch of periodic orbits remains stable until S^0 increases through 9.479. Hence there is stable coexistence of all three species for $8.965 < S^0 < 9.479$. Examples of such stable limit cycles, for different values of S^0, are shown in Figure 10(d).

Note that Figure 10(d) shows that at one of the boundaries of the coexistence state, $S^0 = 9.479$, a Neimark-Sacker is detected, and hence more complex dynamics is likely for $S^0 > 9.479$.

Finally, we note that this is an example of competitor-mediated coexistence. For $8.965 \leq S^0 \leq 9.479$, all three species coexist. However, x_3 cannot survive in the presence of x_2 unless x_1 is also present.

5 Discussion Clearly, the fact that the yield may vary with the nutrient concentration has profound implications for coexistence of several microbial species. The principle of competitive exclusion states that at most one species can survive on a single nutrient at steady state. If one of the competitors exhibits a variable yield, then oscillatory coexistence of more than one species becomes possible.

We have presented one scenario in which the variable yield resulted in the coexistence of two species. Variable yield of the stronger competitor x was beneficial to the weaker competitor y. Specifically, we demonstrated that if the stronger competitor x has a variable yield which generates a stable limit cycle in the plane $y = 0$, than the limit cycle can bifurcate into the coexistence region so that both x and y can stably coexist in oscillatory fashion. Interestingly, a weaker competitor can also benefit if its own yield is variable. If x is a weaker competitor than y at steady state and x exhibits variable yield, then it is possible that both the steady state with $x = 0$ and the limit cycle with $y = 0$ are stable and therefore the outcome of competition will depend on the initial conditions. This is a clear benefit to the weaker competitor x

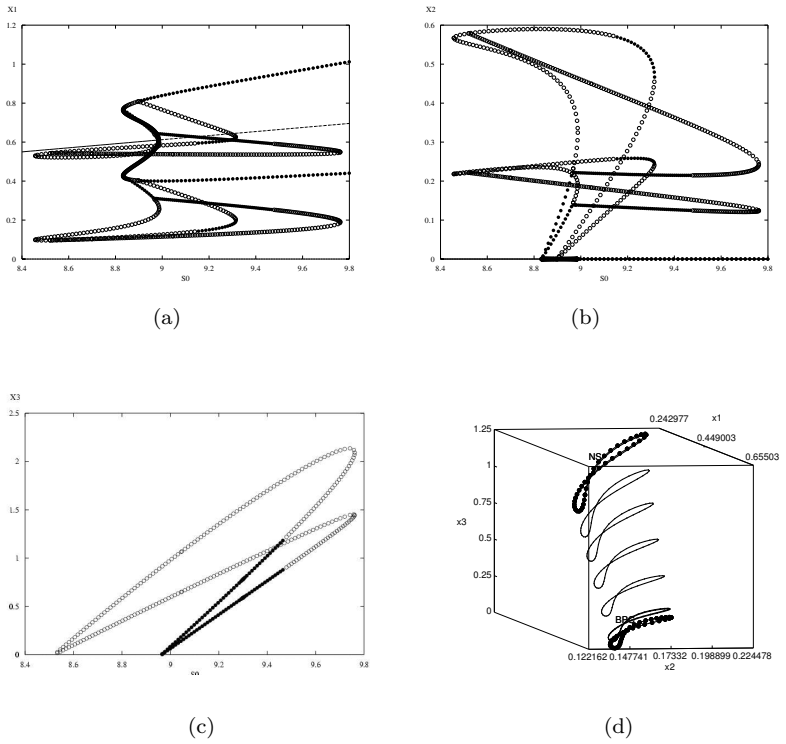

FIGURE 10: (a)-(c) Bifurcation diagrams showing branches where $x_i \geq 0,\ i = 1, 2, 3$. There is stable coexistence of all three species for $8.965 < S^0 < 9.479$. (a) x_1 on the ordinate axis, (b) x_2 on the ordinate axis, (c) x_3 on the ordinate axis. (d) Three species stable oscillatory coexistence for a range of values $8.965 < S^0 < 9.479$. This figure was done using CONTENT (see [**26**]). At $S^0 = 8.965$, a branch point is detected corresponding to a transcritical bifurcation of limit cycles, and at $S^0 = 9.479$, a Neimark-Sacker bifurcation is detected.

because it enables x to outcompete y for some open nonempty set of initial conditions. The second scenario corresponds to bistability.

We also demonstrated that three species coexistence in this context is possible and that competitor-mediated coexistence can occur. In this case, two competitors x_2 and x_3 with fixed yields, a situation that would

normally lead to competitive exclusion, are lead to coexistence by the intervention of a third competitor with variable yield, x_1. The latter acts as a mediator, causing oscillations in the substrate density that make the value of S alternatively beneficial for x_2 and x_3.

In addition to facilitating oscillatory coexistence, the model with variable yield can display much more complicated dynamics. We have presented several examples of dynamically nontrivial attractors corresponding to coexistence (long periodic orbits, invariant tori, linked stable periodic orbits). In a special limiting case, model (15) can exhibit intermittent trajectories if the break-even concentrations of x and y are sufficiently close.

We also explained why it is important to understand how the yield depends on the substrate in order to incorporate the term correctly in the model. In any model in which the yield is considered a measure of the efficacy of the conversion process, the growth and uptake terms are related by the equation $g(S) = Y(S)u(S)$. In order for such a single species growth model to exhibit a Hopf bifurcation, the uptake rate $u(S)$ must be decreasing at high substrate concentrations. In formulating such a model, one therefore must assume that uptake of the substrate is inhibited by high concentrations of substrate. This observation may prove important if one is actually going to try to find organisms in order to observe this phenomenon in the laboratory.

Appendix – Proof of Theorem 2.6 Equation (8) is the transversality condition.

Let $\omega_0 = \sqrt{x^* u(S^*) g'(S^*)}$, denote the imaginary part of the eigenvalue at the critical value α_c, of the Hopf bifurcation parameter. Take

$$T = \begin{bmatrix} 0 & -1 \\ \dfrac{\omega_0}{u(S^*)} & 0 \end{bmatrix} \qquad \text{and} \qquad T^{-1} = \begin{bmatrix} 0 & \dfrac{u(S^*)}{\omega_0} \\ -1 & 0 \end{bmatrix},$$

$$\begin{pmatrix} r \\ v \end{pmatrix} = T^{-1} \begin{pmatrix} S \\ x \end{pmatrix} \Longrightarrow \begin{cases} r = x \dfrac{u(S^*)}{\omega_0} \\ v = -S \end{cases}.$$

Thus, in canonical form the system is

$$\frac{dr}{dt} = r(-D_1 + g(-v)) \equiv f(r, v),$$

$$\frac{dv}{dt} = -(S^0 + v)D + r\frac{\omega_0}{u(S^*)} u(-v) \equiv g(r, v).$$

Now the system is in the canonical form so that a straight forward application of the formula in Marsden and McCracken [**34**] shows that the sign of $\mathcal{C}_H$ determines the criticality of the Hopf bifurcation as indicated in Theorem 2.6.

Alternatively, defining $h(s) = D(S^0 - S)/u(S)$, one can write the system (1) in the form:

$$\frac{dS}{dt} = \left(\frac{D(S^0 - S)}{u(S)} - x\right) u(S) \equiv (h(S) - x)u(S),$$
$$\frac{dx}{dt} = (g(S) - D_1)\, x.$$

In [**44**] the criterion for the criticality of the Hopf bifurcation based on the sign of $\widehat{\mathcal{C}}_H$ was derived.

REFERENCES

1. B. J. Abbott and A. Clamen, *The relationship of substrate, growth rate, and maintenance coefficient to single cell protein production*, Biotechnology and Bioengineering **15** (1973), 117–127.
2. P. Agrawal, C. Lee, H. C. Lim and D. Ramkrishna, *Theoretical investigations of dynamic behavior of isothermal continuous stirred tank biological reactors*, Chemical Engineering Science **37**(3) (1982), 453-462.
3. J. F. Andrews, *A mathematical model for the continuous culture of microorganisms utilizing inhibitory substrates*, Biotechnology and Bioengineering **10** (1968), 707–723.
4. J. Arino, *Modélisation structurée de la croissance du phytoplancton en chemostat*, Université Grenoble 1, 2001.
5. *Simulating, Analyzing, and Animating Dynamical Systems: A guide to XPPAUT for researhers and students* (B. Ermentrout, ed.), SIAM, Philadelphia, 2002.
6. K. Bandyopadhyay, D. Das and B. R. Maiti, *Kinetics of phenol degradation using* Pseudomonas putida *MTCC 1994*, Bioprocess Engineering **18** (1998), 373–377.
7. G. E. Briggs and J. B. S. Haldane, *A note on the kinetics of enzyme action*, Biochem. J. **19** (1925), 338–339.
8. G. J. Butler and P. Waltman, *Bifurcation from a limit cycle in a two predator-one prey ecosystem modeled on a chemostat*, J. Math. Biol. **12** (1981), 295–310.
9. G. J. Butler and G. S. K. Wolkowicz, *A mathematical model of the chemostat with a general class of functions describing nutrient uptake*, SIAM J. Appl. Math. **45**(1) (1985), 138–151.
10. *Continuous Cultures of Cells* (P. H. Calcott, ed.), CRC Press, 1981.
11. P. Crooke and R. Tanner, *Hopf bifurcations for a variable yield continuous fermentation model*, Int. J. Engng. Sci. **20**(3) (1982), 439–443.
12. P. Crooke, C.-J. Wei and R. Tanner, *The effect of the specific growth rate and yield expressions on the existence of oscillatory behavior of a continuous fermentation model*, Chem. Eng. Commun. **6** (1980), 333–347.

13. E. P. Dahlen and B. E. Rittmann, *Analysis of oxygenation reactions in a multi-substrate system – A new approach for estimating substrate-specific true yields*, Biotechnology and Bioengineering **70**(6) (2000), 685–692.
14. G. Dinopoulou, R. M. Sterritt and J. N. Lester, *Anaerobic acidogenesis of a complex wastewater: II. Kinetics of growth, inhibition, and product formation*, Biotechnology and Bioengineering **31** (1988), 969–978.
15. A. G. Dorofeev, M. V. Glagolev, T. F. Bondarenko and N. S. Panikov, *Observation and explanation of the unusual growth kinetics of Arthrobacter globiformis*, Microbiology **61** (1992), 24–31.
16. V. H. Edwards, *The influence of high substrate concentrations on microbial kinetics*, Biotechnology and Bioengineering **12** (1970), 679–712.
17. C. K. Essajee and R. D. Tanner, *The effect of extracellular variables on the stability of the continuous baker's yeast-ethanol fermentation process*, Process Biochemistry, 1979.
18. F. B. Godin, D. G. Cooper and A. D. Rey, *Development and solution of a cell mass population balance model applied to the SCF process*, Chemical Engineering Science **54** (1999), 565–578.
19. M. T. Flikweert, M. Kuyper, A. J. A. van Maris, P. Kötter, J. P. van Dijken and J. T. Pronk, *Steady-state and transient-state analysis of growth and metabolite production in a* Saccharomyces cerevisiae *strain with reduced pyruvate-decarboxylase activity*, Biotechnology and Bioengineering **66**(1) (1999), 42–50.
20. S. R. Hansen and S. P. Hubbell, *Single-Nutreint Microbial Competition: Qualitative Agreement Between Experimental and Theoretically Forecast Outcomes*, Science **207** (1980), 1491–1493.
21. G. P. Harrison, *Global stability of predator-prey interactions*, J. Math. Biol. **8** (1979), 159–171.
22. R. Heidemann, D. Lütkemeyer, H. Büntemeyer and J. Lehmann, *Effects of dissolved oxygen levels and the role of extra- and intracellular amino acid concentrations upon the metabolism of mammalian cell lines during batch and continuous cultures*, Cytotechnology **26** (1998), 185–197.
23. S. B. Hsu, *Limiting behavior for competing species*, SIAM J. Appl. Math. **34** (1978), 760–763.
24. S. Koga and A. E. Humphrey, *Study of the dynamic behavior of the chemostat system*, Biotechnology and Bioengineering **9** (1967), 375–386.
25. U. Kulozik, *Physiological aspects of continuous lactic acid fermentations at high dilution rates*, Appl. Microbiol. Biotechnol. **49** (1998), 506–510.
26. *CONTENT - Integrated Environment for Analysis of Dynamical Systems* (Y. A. Kuznetsov, ed.), Report, UPMA-98-224, École Normale Superioure de Lyon, Lyon, France, 1998.
27. I. H. Lee, A. G. Fredrickson and H. M. Tsuchiya, *Damped oscillations in continuous culture of* Lactobacillus plantarum, Journal of General Microbiology **93** (1976), 204–208.
28. F. Lei, L. Olsson and S. B. Jorgensen, *Experimental investigations of multiple steady states in aerobic continuous cultivations of* Saccharomyces cerevisiae, Biotechnology and Bioengineering **82**(7) (2003), 766–777.
29. Y. Lenbury, P. S. Crooke and R. D. Tanner, *Relating damped oscillations to sustained limit cycles describing real and ideal batch fermentation processes*, BioSystems **19** (1986), 15–22.
30. B. Li, *Global asymptotic behavior of the chemostat: general response functions and differential death rates*, SIAM J. Appl. Math. **59** (1999), 411–422.
31. H. Y. Lin, Bayrock and Ingledew, *Evaluation of* Saccharomyces cerevisiae *grown in a multistage chemostat environment under increasing levels of glucose*, Biotechnology Letters **24** (2002), 449–453.

32. J. E. Littlewood, *A mathematician's miscellany*, Methuen and Co., London, 1953.
33. J. H. T. Luong, *Generalization of Monod kinetics for analysis of growth data with substrate inhibition*, Biotechnology and Bioengineering **29** (1987), 242–248.
34. J. E. Marsden and M. McCracken, *The Hopf Bifurcation and its Applications*, Springer, 1976.
35. J. Monod, *The growth of bacterial cultures*, Annual Review of Microbiology **3** (1949), 371–394.
36. A. Moser, *Bioprocess Technology*, Springer, 1988.
37. S. S. Pilyugin and P. Waltman, *Multiple limit cycles in the chemostat with variable yield*, Math. Biosciences **182** (2003), 151–166.
38. S. S. Pilyugin and P. Waltman, *Divergence criterion for generic planar systems*, SIAM J. Appl. Math. **64**(1) (2003), 81–93.
39. S. C. Ricke and D. M. Schaefer, *Growth and fermentation responses of* Selenomonas ruminantium *to limiting and non-limiting concentrations of amonium chloride*, Appl. Microbiol. Biotechnol. **46** (1996), 169–175.
40. N. S. Rao and E. O. Roxin, *Controlled growth of competing species*, SIAM J. Appl. Math. **50**(3) (1990), 853–864.
41. H. L. Smith and P. Waltman, *The theory of the chemostat*, Cambridge University Press, 1995.
42. J. M. VanBriesen, *Evaluation of methods to predict bacterial yield using thermodynamics*, Biodegradation **13** (2002), 171–190.
43. J. L. Webb, *Enzyme and Metabolic Inhibitors. Volume I. General Principles of Inhibition*, Academic Press, 1963.
44. G. S. K. Wolkowicz, *Bifurcation analysis of a predator-prey system involving group defense*, SIAM J. Appl. Math. **48**(3) (1988), 592–606.
45. G. S. K. Wolkowicz and Z. Lu, *Global dynamics of a mathematical model of competition in the chemostat: general response functions and differential death rates*, SIAM J. Appl. Math. **52**(1) (1992), 222–233.
46. G. S. K. Wolkowicz and H. Xia, *Global asymptotic behavior of a chemostat model with discrete delays*, SIAM J. Appl. Math. **57**(4) (1997), 1019–1043.
47. H. Zhu, S. A. Campbell and G. S. K. Wolkowicz, *Bifurcation analysis of a predator-prey system with nonmonotonic functional response*, SIAM J. Appl. Math. **63**(2) (2002), 636–682.

Department of Mathematics, McMaster University, Hamilton, ON, Canada L8S 4K7

Department of Mathematics, University of Florida, Gainesville, FL 32611-8105, USA

Department of Mathematics, McMaster University, Hamilton, ON, Canada L8S 4K7